Supporting information

Observation of the Bending Mode of Interfacial Water at Silica Surfaces by Near Infrared Vibrational Sum-frequency Generation Spectroscopy of the [stretch+bend] Combination Bands

Oleksandr Isaienko, Satoshi Nihonyanagi, Devika Sil and Eric Borguet
Department, Temple University
1901 North 13th Street, Philadelphia, Pennsylvania, 19122 USA

1. Calculation of the IR Fresnel factor $L_{zz}(IR)$.

The intensity of sum-frequency signal is determined, among other parameters, by the effective nonlinearity of the interface $\chi^{(2)}_{eff}$ and the intensities of the input beams $I(\omega_{IR})$ and $I(\omega_{VIS})$ [1]:

$$I(\omega_{SFG}) = \frac{8\pi^3 \omega_{SFG}^{\ 2} \sec^2 \beta_{SFG}}{c^3 n_1(\omega_{IR}) n_1(\omega_{VIS}) n_1(\omega_{SFG})} \left|\chi^{(2)}_{eff}\right|^2 I(\omega_{IR}) I(\omega_{VIS}) . \quad (1)$$

Here, $n_1(\omega_x)$ is the index of refraction of beam at the corresponding frequency ω_x in medium 1, β_{SFG} is the angle of reflection for the SF-beam, c is the speed of light. The non-zero components of the $\chi^{(2)}$-tensor define the corresponding second-order susceptibilities for each polarization combination, according to the following expressions [1, 2]:

$$\chi^{(2)}_{eff,SSP} = L_{yy}(\omega_{SFG}) L_{yy}(\omega_{VIS}) L_{zz}(\omega_{IR}) \sin\theta_{IR} \chi_{yyz} , \quad (2)$$

$$\chi^{(2)}_{eff,SPS} = L_{yy}(\omega_{SFG}) L_{zz}(\omega_{VIS}) L_{yy}(\omega_{IR}) \sin\theta_{VIS} \chi_{yzy} , \quad (3)$$

$$\chi^{(2)}_{eff,PSS} = L_{zz}(\omega_{SFG}) L_{yy}(\omega_{VIS}) L_{yy}(\omega_{IR}) \sin\theta_{SFG} \chi_{zyy} , \quad (4)$$

$$\begin{aligned} \chi^{(2)}_{eff,PPP} = {} & L_{xx}(\omega_{SFG}) L_{xx}(\omega_{VIS}) L_{zz}(\omega_{IR}) \cos\theta_{SFG} \cos\theta_{VIS} \sin\theta_{IR} \chi_{xxz} \\ & - L_{xx}(\omega_{SFG}) L_{zz}(\omega_{VIS}) L_{xx}(\omega_{IR}) \cos\theta_{SFG} \sin\theta_{VIS} \cos\theta_{IR} \chi_{xzx} \\ & + L_{zz}(\omega_{SFG}) L_{xx}(\omega_{VIS}) L_{xx}(\omega_{IR}) \sin\theta_{SFG} \cos\theta_{VIS} \cos\theta_{IR} \chi_{zxx} \\ & + L_{zz}(\omega_{SFG}) L_{zz}(\omega_{VIS}) L_{zz}(\omega_{IR}) \sin\theta_{SFG} \sin\theta_{VIS} \sin\theta_{IR} \chi_{zzz} \end{aligned} \quad (5)$$

Here, θ_i are the incidence angles for the corresponding beams (i=VIS, or IR), while the parameters $L_{xx}(\omega_i)$, $L_{yy}(\omega_i)$, $L_{zz}(\omega_i)$ are the Fresnel factors for each of the interacting beams. The Fresnel coefficients are given by the following expressions [3]:

$$L_{xx}(\omega_i) = \frac{2 n_1(\omega_i) \cos\gamma_i}{n_1(\omega_i)\cos\gamma_i + n_2(\omega_i)\cos\theta_i} , \quad (6)$$

$$L_{yy}(\omega_i) = \frac{2 n_1(\omega_i) \cos\theta_i}{n_1(\omega_i)\cos\theta_i + n_2(\omega_i)\cos\gamma_i} , \quad (7)$$

$$L_{zz}(\omega_i) = \frac{2 n_2(\omega_i) \cos\theta_i}{n_1(\omega_i)\cos\gamma_i + n_2(\omega_i)\cos\theta_i} \left(\frac{n_1(\omega_i)}{n_M(\omega_i)}\right)^2 . \quad (8)$$

In Eqns. 6-8, θ_i is the angle of incidence of the wave at frequency ω_i; $n_1(\omega_i)$ and $n_2(\omega_i)$ are the indices of refraction of media 1 and 2 for the corresponding waves; γ_i is the angle of refraction of the corresponding wave in medium 2 ($n_2(\omega_i)\sin\gamma_i = n_1(\omega_i)\sin\theta_i$); $n_M(\omega_i)$ is the index of refraction of the

interfacial intermediate layer at the boundary between media 1 and 2. To estimate the index of refraction of the intermediate layer n_M, the following relation was suggested and successfully applied [1]:

$$(n_M(\omega_i))^2 = (n_1(\omega_i))^2 \cdot \frac{|n_2(\omega_i)|^2 \left(|n_2(\omega_i)|^2 + 5\right)}{4|n_2(\omega_i)|^2 + 2}. \qquad (9)$$

For the case of the incidence angles close to the respective critical values, $\gamma_{VIS} \approx \gamma_{IR} \approx 90^o$, thus $\cos\gamma_{VIS} \approx \cos\gamma_{SFG} \approx 0$ ($\cos\gamma_{IR}$ may be a complex value, see below), and in turn coefficients $L_{xx}(\omega_i)$ become close to zero (Eqn. 6). In these particular conditions, the SF-signal in ppp-combination is simplified to [3]:

$$\chi^{(2)}{}_{eff,PPP} \approx L_{zz}(\omega_{SFG}) L_{zz}(\omega_{VIS}) L_{zz}(\omega_{IR}) \sin\theta_{SFG} \sin\theta_{VIS} \sin\theta_{IR} \chi_{zzz}. \qquad (10)$$

We get the following expressions for the Fresnel factors for the SFG, VIS and IR beams that contribute the most in the ppp-polarization respectively (assuming that the VIS and SFG beams are at the critical angle; the IR angle is varied):

$$L_{zz}(\omega_{SFG}) = 2\left(\frac{n_1(\omega_{SFG})}{n_M(\omega_{SFG})}\right)^2 \qquad (11)$$

$$L_{zz}(\omega_{VIS}) = 2\left(\frac{n_1(\omega_{VIS})}{n_M(\omega_{VIS})}\right)^2 \qquad (12)$$

$$L_{zz}(\omega_{IR}) = \frac{2\left[n'_2(\omega_{IR}) + in''_2(\omega_{IR})\right]\cos\theta_{IR}}{n_1(\omega_{IR})\cos\gamma_{IR} + \left[n'_2(\omega_{IR}) + in''_2(\omega_{IR})\right]\cos\theta_{IR}} \frac{(n_1(\omega_{IR}))^2}{(n_M(\omega_{IR}))^2} \qquad (13)$$

Here, $n'_2(\omega_{IR})$ and $n''_2(\omega_{IR})$ are the real and imaginary parts of bulk water's index of refraction, respectively, which can be obtained by fitting the data from the literature [4, 5] (Fig. S1). The index of refraction of silica was calculated using the Sellmeier coefficients from the reference literature [6].

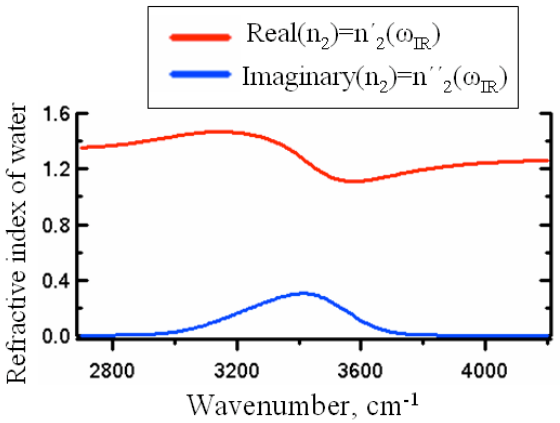

Fig. S1. The real (red) and imaginary (blue) parts of the bulk water index of refraction based on the fits of the experimental data [4].

Based on Eqns. 11-13, we calculate the Fresnel factors for the three beams for the geometry settings (incidence angles ~67° for visible, ~75° for IR). The Fresnel factors for vis and SFG beams are practically constant, while the infrared Fresnel factor varies significantly in the 3000-4000 cm^{-1} range due to water absorption (Fig. S2) [5]. Thus, only the latter factor was used to additionally normalize the SFG spectra from silica/water interfaces.

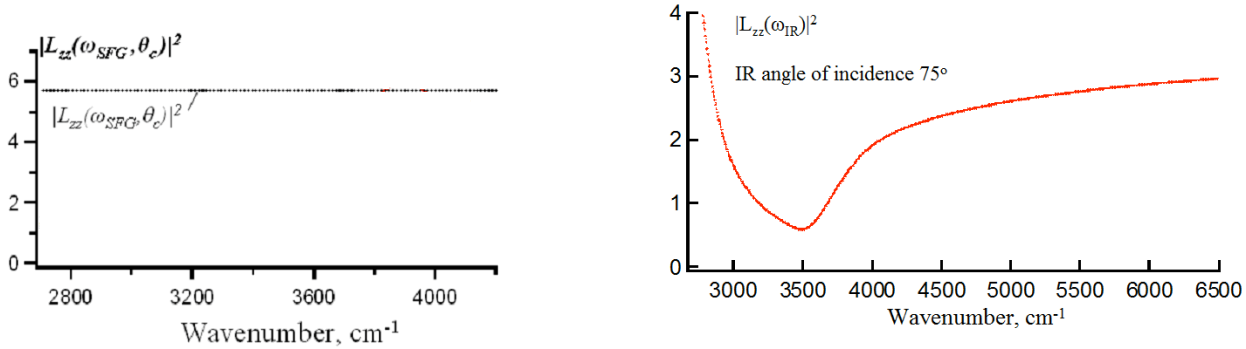

Fig. S2. Modulus square values for the Fresnel factors of SFG (left) and IR (right) beams calculated for silica/water interface following Eqns. 11-13.

2. Sample preparation for SFG spectroscopy; spectral acquisition.

The silica/water interface was created by placing IR-grade fused silica (IRFS) hemicylinder prisms on top of aqueous solutions placed into Teflon holder.[7] The infrared-grade fused silica prisms used for the broadband vibrational spectroscopy of mineral/water interfaces were prepared by cleaning in "piranha" cleaning solution which is 1 vol. conc. H_2O_2: 3 vol. conc. H_2SO_4 (*CAUTION: "piranha" is a very reactive and corrosive mixture! It must be handled with a great care; use of protective equipment such as gloves, eye goggles and labcoat is mandatory.*). Water was obtained from a Thermoscientific Barnstead Easypure II purification system equipped with a UV lamp; final water resistivity ~18 MOhm·cm. Acidic solutions were prepared by diluting as received concentrated HCl (12.1 normal, Fisher Scientific grade, Certified ACS Plus) in deionized H_2O. Basic solutions were prepared by diluting as received 4 M standard solution of NaOH (Fluke Analytical). The values of pH of the prepared solutions were verified with a pH-meter (Oacton). Solutions of varying salt concentration were prepared by dissolving as received NaCl crystals (Fisher Scientific, >99.8%) in neutral deionized H_2O.

The SFG spectra of the water combination band were acquired in ppp-polarization scheme (beams SFG, VIS and IR p-polarized at the interface). The detection sensitivity for SFG in ssp configuration has yet to be improved for the combination band range as the signal remained buried in the noise even after few minutes of CCD integration time; the fundamental OH stretch peaks, however, were clearly measured in ssp.

3. Calibration of sum-frequency scale in the combination band region.

The acquisition of the sum-frequency spectra in the near-IR range required calibration of the wavenumber scale. In this case, a 2-mm pathlength quartz cuvette filled with n-butanol was used as a calibration sample (similar to the empty quartz cuvette for calibration in the ~3000 – 4000 cm^{-1} region [7]). This sample has a relatively strong absorption peak at 4780 cm^{-1} (Fig. S3) corresponding to the combination band of the OH stretch and bending of the C-O-H group in the alcohol [8].

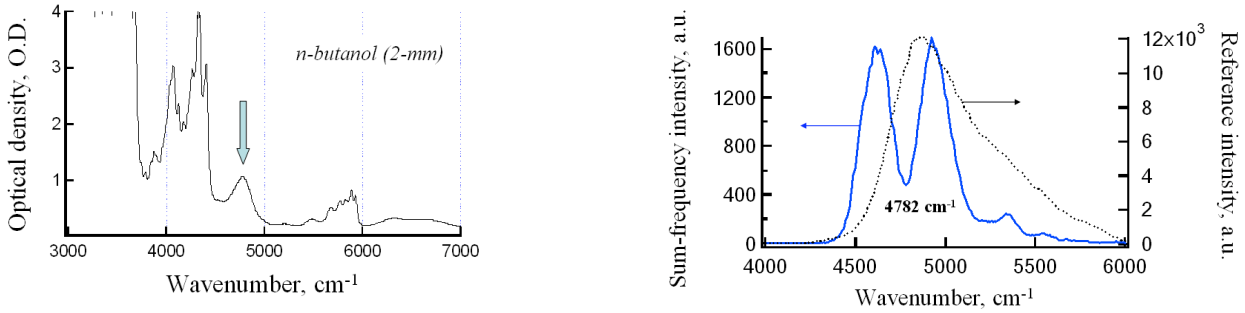

Fig. S3. Calibration of sum-frequency scale in the combination band range. Left: FTIR spectrum of the calibration sample (~2-mm path of n-butanol in a quartz cell). The arrow points at the peak used for calibration (bending+OH-stretch combination of the C-O-H group, 4779 cm^{-1} [8]). Right: SFG spectrum on gold/fused silica prism with the calibration sample in the IR beam path (with the actual position of the dip in SFG spectrum). The shifts in the experimental position of the dip from the expected frequency varied from ~+5 cm^{-1} to ~+20-25 cm^{-1}.

4. Acquisition of FTIR and Raman spectra

For IR absorption spectral measurements, we used a Bruker FTIR spectrometer, model Tensor 27 with DTGS external detector. A thin layer of liquid water was created by squeezing water between two Menzel silica coverslips; FTIR spectra were measured against the background of two glass coverslips without water in-between. Spectra were measured with 4 cm^{-1} resolution, 100 scans.

Raman spectra of liquid water were measured by using excitation at 532 nm (18797 cm^{-1}); the pump beam was obtained from a Verdi-V5 CW laser (Coherent), the beam power was varied in the 0.25-1 W range. The linearity of the Raman scattering signal was ensured by measuring the dependence of the intensity of the OH stretch peaks vs the pump power. Liquid water samples were placed into a 10-mm pathlength quartz cell. The pump beam was focused in the center of the liquid water samples with a 50-mm lens (BK7) and the Raman scattering was collected with a 70-mm, 2-inch diameter lens (BK7). The collimated scattered Raman signal was then focused into the input of an optical fiber with a 50-mm lens (BK7). The polarization of the pump beam at the sample was adjusted with a waveplate; the polarization of Raman scattering was selected with a Glan-Taylor polarizer in front of the fiber input. The fiber transmitted the signal to the Andor spectrometer-CCD system that was used for SFG spectroscopic measurements [7]. The wavelength scale was calibrated using the spectrum from a Hg lamp.

Data analysis of FTIR, Raman and SFG spectra was done with Igor Pro 5.03.

5. Baseline fitting of Raman spectra in the water combination band range.

Fit formula of Igor's built-in multi-peak function:

$$S(\omega) = S_{baseline}(\omega) + \sum S_{peak}(\omega)$$

Log Poly 5 equation of baseline:

$\omega_r = \log(\omega_{end} / \omega_{start})$

$\omega' = (2 \log \omega - \omega_{start} * \omega_{end}) / \omega_r$

$S_{baseline}(\omega) = f(\omega') = k_0 + k_1(\omega') + k_2(\omega')^2 + k_3(\omega')^3 + k_4(\omega')^4 + k_5(\omega')^5$

Formula for Gaussian peak:

$S_{peak1}(\omega) = k_6 \cdot \exp[-(\omega - k_7)^2 / k_8^2]$;

$S_{peak1}(\omega) = k_9 \cdot \exp[-(\omega - k_{10})^2 / k_{11}^2]$;

etc.

Table S1. Coefficients for the fits of Raman spectra in Fig. 3B.

	Baseline coefficients	Coefficients for individual peaks (Gaussian)
VV spectrum	K0 = 5399.1 ± 0 K1 = 1201.6 ± 0 K2 = 170 ± 81 K3 = -146 ± 1.0 10^3 K4 = 878 ± 226 K5 = -1526 ± 2.72 10^3	Peak 1: K6(height) = 94 ± 146 K7(position) = 4900 ± 17 K8(width) = 146 ± 65 Peak 2: K9(height) = 206 ± 82 K10(position) = 5168 ± 17 K11(width) = 179 ± 15
HH spectrum	K0 = 5298 ± 0 K1 = 1404 ± 0 K2 = 253 ± 3 K3 = -657 ± 9 K4 = 1740 ± 18 K5 = -1869 ± 49	K6(height) = 244 ± 3 K7(position) = 5154 ± 2 K8(width) = 182 ± 3

6. FTIR spectrum of liquid water combination band

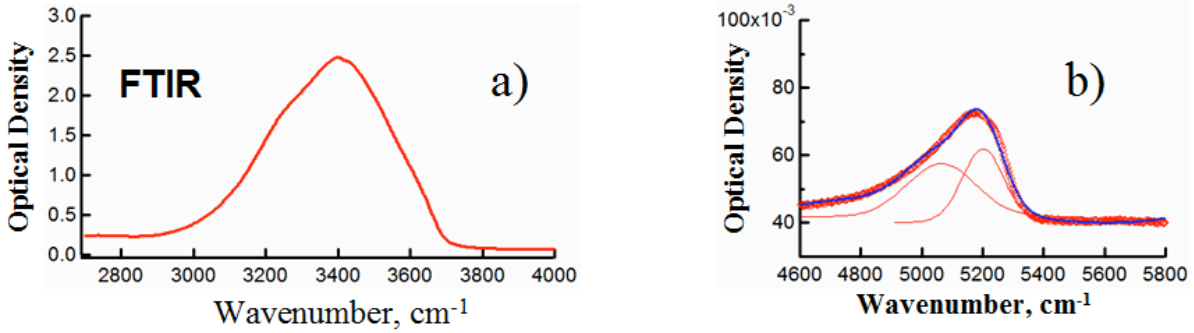

Fig. S4. FTIR spectrum of thin water (H_2O) layer in the fundamental (a) and combination band (b) frequency ranges. In (b), blue line is a two-peak fit.

Table S2. Fit results for the water combination band IR spectrum (Fig. S4).

Spectrum	Baseline coefficients	Coefficients for individual peaks (Gaussian)
	K0 = 5201.3 ± 0 K1 = 1199.6 ± 0 K2 = 0.0434 ± 0.0003 K3 = -0.015 ± 0.001 K4 = -0.00062 ± 0.0015 K5 = 0.045 ± 0.005	Peak 1: K6(height) = 0.0157 ± 0.0013 K7(position) = 5064 ± 17 K8(width) = 159 ± 14 Peak 2: K9(height) = 0.0216 ± 0.003 K10(position) = 5201 ± 2 K11(width) = 96 ± 4

7. Fit parameters for SFG spectra from neat H_2O/silica and pH2/silica surfaces.

The SFG spectra from neat H_2O/silica surface in the fundamental OH stretch range (~3000-4000 cm^{-1}) could be fit with either pure Lorentzians, or with inhomogenously broadened Lorentzians following Eqn. (S1) below (see Table S3 for fit results):

$$\chi^{(2)} = \chi_{NR}{}^{(2)} \cdot \exp(i\varphi_{NR}) + \sum_j \int d\omega_j \frac{B_j}{\omega - \omega_j + i\Gamma_j} \cdot \exp\left(-\frac{(\omega_j - \omega_{j0})^2}{\sigma_j^2}\right) \qquad \text{(S1)}$$

The values of the nonresonant nonlinearity χ_{NR} and the relative phase offset φ_{NR} between the resonant and nonresonant contributions were extracted from the signal levels around 4000-4500 cm^{-1} where the interferences between the tails of the OH peaks and the nonresonant nonlinearity are observed with our SFG spectrometer [7] directly. In some fits, certain values were kept fixed, mostly the parameters for OH stretches in the fits of the combination band SFG response.

Table S3. Fit parameters for data in Figures 1(A,B) and 3A. Zero fit errors indicate values preset for some parameters based on the results of previous fits.

Spectrum	χ_{NR}, a.u.	φ_{NR}, rad	Oscillator strengths B_j, (a.u.)	Center frequencies ω_{j0} (cm^{-1})	Natural linewidths Γ_j, (cm^{-1})	Gaussian broadening σ_j (cm^{-1})
Neat H_2O/silica; 3000-4000 cm^{-1} range (Fig. 1,a)	0.009 (fixed)	-0.23 (fixed)	19.0 ± 0.3 -12 ± 1 -5.3 ± 0.9	3160 ± 2 3493 ± 3 3643 ± 9	10 ± 0 10 ± 0 10 ± 0	142 ± 2 90 ± 3 99 ± 12
Neat H_2O/silica; 4500-5800 cm^{-1} range (Fig. 1,a) – fit by Eqn S2	0.009 (fixed)	-0.23 (fixed)	40 ± 5 -38 ± 3 -2.5 ± 0 -0.111± 0.131 0.362 ± 0.06	3135 ± 0 3478 ± 0 3656 ± 0 5060± 0 (fixed) 5325± 8.6	135.51 ± 0 96 ± 352 73.2 ± 0 135± 99 115± 15	N/A 2019 ± 283 N/A N/A N/A
pH2/silica; 3000-5800 cm^{-1} (Figs. 1, a,b,d)	0.008 (fixed)	-0.277 (fixed)	17± 0 -6.06± 0 -6.34± 0 -0.024 ± 0.015 0.066 ± 0.016	3165.1± 0 3501.4± 0 3667.5± 0 5061 ± 55 5360 ± 18.3	200± 0 10± 0 119± 0 5± 0 5± 0	10± 0 101.44± 0 1± 0 90± 0 86 ± 26

For SFG spectra from neat H_2O/silica in the combination band frequency range it was found that the OH stretch peaks contribute significantly with their "tails" interfering with each other and thus dictating the SFG signal levels in the ~4500-5800 cm^{-1} range. Thus the contribution of the OH peak tails had to be modeled somehow. We found that it was rather challenging to fit the neat H_2O/silica SFG spectra over the entire 3000-5800 cm^{-1} range simultaneously with the OH peaks modeled as inhomogeneously broadened Lorentzians (Eqn. S1). The latter can be explained by the fact that we are attempting to fit simultaneously SFG spectra over the two frequency ranges that were measured under different conditions. However, the OH stretch contribution (namely, the slope of the SFG spectra at ~5000 cm^{-1} due to OH peaks) in the near-IR could be modeled when the 3480 cm^{-1} peak was multiplied by a Gaussian of a certain width while modeling the other peaks as Lorentzians; in this case, essentially the Voigt profile of the 3480 cm^{-1} peak was modeled as a product of Lorentzian and Gaussian functions:

$$\chi^{(2)} = \chi_{NR}^{(2)} \cdot e^{i\varphi_{NR}} + \sum_k \frac{B_k}{\omega - \omega_k + i\Gamma_k} + \frac{B_{3480}}{\omega - \omega_{3480} + i\Gamma_{3480}} \cdot \exp\left(-\frac{(\omega - \omega_{3480})^2}{\sigma_{3480}^2}\right). \qquad \text{(S2)}$$

The frequency of the 5060 cm^{-1} peak was fixed to the value found from the fits of SFG spectra from pH2/silica (see below); otherwise, the fitting procedure could not locate the feature due to its weakness compared to the 5300 cm^{-1} peak, as well as the fact that it was largely "hidden" by the high slope of SFG signal due to strong contribution from OH peaks.

As the pH of aqueous phase decreased to ~2, the OH stretch peaks showed much less contribution in the near-IR and the sum-frequency spectra in both frequency ranges could be fit simultaneously with Eqn. S1 (Eqn. 1 in the manuscript). In this case, both combination band features were clearly observed.

8. Simulation of zero-crossing in SFG spectra from neat H_2O/silica interface.

Below we demonstrate that the zero-crossing in SFG spectra from water/silica surfaces around 4300 cm^{-1} can occur only for the relative phase φ_{NR} values close to 0 (or $\pm\pi$). We use Eqn. S1 to simulate the SFG spectra in both 3000-4000 and 4000-5000 cm^{-1} ranges based on the three OH peaks (Table S3).

Table S4. Peak parameters for simulated SFG spectra in Figure S5.

Spectrum	χ_{NR}, a.u.	φ_{NR}, rad	Oscillator strengths B_i, (a.u.)	Center frequencies ω_{i0} (cm^{-1})	Natural linewidths Γ_i, (cm^{-1})	Gaussian broadening σ_i (cm^{-1})
Neat H_2O/silica; Spectrum (a)	0.009	0	19.046 -11.65 -5.2787	3160.2 3492.5 3642.5	10 10 10	142.42 90.2 99.435
Neat H_2O/silica; Spectrum (b)	0.009	$\pi/2$	19.046 -11.65 -5.2787	3160.2 3492.5 3642.5	10 10 10	142.42 90.2 99.435
Neat H_2O/silica; Spectrum (c)	0.009	$-\pi/2$	19.046 -11.65 -5.2787	3160.2 3492.5 3642.5	10 10 10	142.42 90.2 99.435
Neat H_2O/silica; Spectrum (d)	0.009	$\pi/2$	-19.046 11.65 5.2787	3160.2 3492.5 3642.5	10 10 10	142.42 90.2 99.435
Neat H_2O/silica; Spectrum (e)	0.009	$-\pi$	-19.046 11.65 5.2787	3160.2 3492.5 3642.5	10 10 10	142.42 90.2 99.435

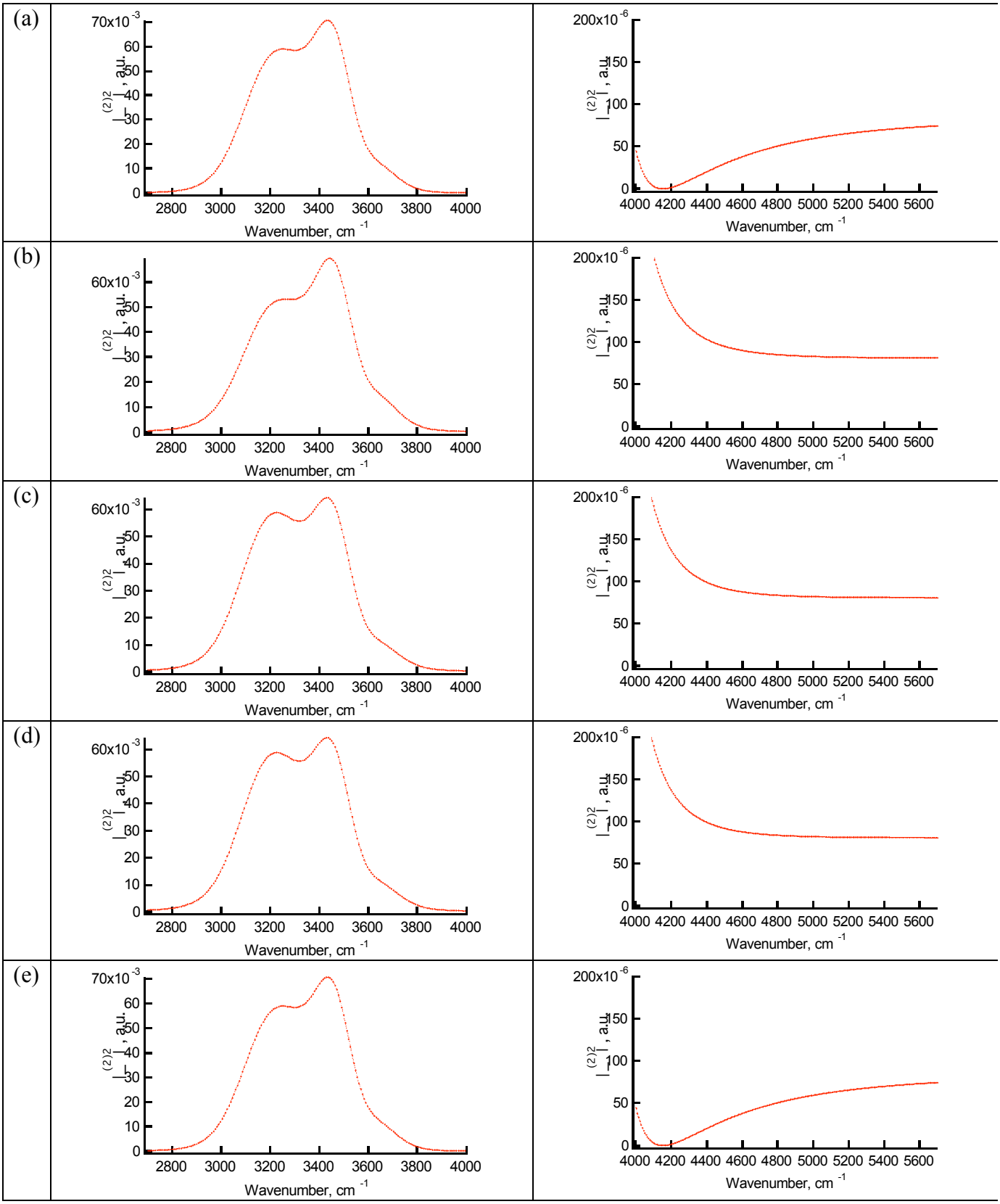

Fig. S5. Simulations of SFG spectra based on parameters in Table S4.

References:

1. Zhuang, X., Miranda, P.B., Kim, D., and Shen, Y.R., *Mapping molecular orientation and conformation at interfaces by surface nonlinear optics.* Physical Review B **59**(19), 12632-12640 (1999)
2. Gan, W., Wu, D., Zhang, Z., Feng, R.R., and Wang, H.F., *Polarization and experimental configuration analyses of sum frequency generation vibrational spectra, structure, and orientational motion of the air/water interface.* Journal of Chemical Physics **124**(11), 114705 (2006)
3. Lobau, J. and Wolfrum, K., *Sum-frequency spectroscopy in total internal reflection geometry: Signal enhancement and access to molecular properties.* Journal of the Optical Society of America B-Optical Physics **14**(10), 2505-2512 (1997)
4. Bertie, J.E., Ahmed, M.K., and Eysel, H.H., *Infrared intensities of liquids .5. optical and dielectric-constants, integrated-intensities, and dipole-moment derivatives of h2o and d2o at 22-degrees-c.* Journal of Physical Chemistry **93**(6), 2210-2218 (1989)
5. York, R.L., Li, Y.M., Holinga, G.J., and Somorjai, G.A., *Sum frequency generation vibrational spectra: The influence of experimental geometry for an absorptive medium or media.* Journal of Physical Chemistry A **113**(12), 2768-2774 (2009)
6. Tropf, W.J., Thomas, M.E., and Harris, T.J., *Properties of crystals and glasses*, in *Handbook of optics*, M. Bass, Editor. 1995, McGraw-Hill: New York. p. 33.3-33.83.
7. Isaienko, O. and Borguet, E., *Ultra-broadband sum-frequency vibrational spectrometer of aqueous interfaces based on a non-collinear optical parametric amplifier.* Opt. Express **20**(1), 547-561 (2012)
8. Workman, J. and Weyer, L., *Practical Guide to Interpretive Near-Infrared Spectroscopy*. 2007, Boca Raton, FL: CRC Press.